Cholesterol reduction by methyl-β-cyclodextrin attenuates the delta opioid receptor-mediated signaling in neuronal cells but enhances it in non-neuronal cells

Peng Huang [a], Wei Xu [a], Su-In Yoon [b], Chongguang Chen [a], Parkson Lee-Gau Chong [b], Lee-Yuan Liu-Chen [a],*

[a] Department of Pharmacology, Center for Substance Abuse Research, Temple University School of Medicine, 3420 N Broad Street, Philadelphia, PA 19140, United States
[b] Department of Biochemistry, Center for Substance Abuse Research, Temple University School of Medicine, 3420 N Broad Street, Philadelphia, PA 19140, United States

ARTICLE INFO

ABSTRACT

Opioid receptors have been shown to be located in and regulated by lipid rafts/caveolae in caveolin-rich non-neuronal cells. Here, we found that caveolin-1 level was very low in rat brain and undetectable in NG108-15 cells, which endogenously express delta opioid receptors (DOR). Rat caudate putamen (CPu) membranes, NG108-15 cells and CHO cells stably transfected with FLAG-mouse-DOR (CHO-FLAG-mDOR) were homogenized, sonicated in a detergent-free 0.5 M Na_2CO_3 buffer and fractionated through discontinuous or continuous sucrose density gradients. About 70% of opioid receptors in CPu and DOR in both cell lines were present in low-density (5–20% sucrose) membrane domains enriched in cholesterol and ganglioside M1 (GM1), characteristics of lipid rafts in plasma membranes. In both cells, stimulation with permeable or non-permeable full agonists, but not with partial or inverse agonists, for 30 min shifted ~25% of DORs out of rafts, by a naloxone-reversible and pertussis toxin-insensitive mechanism, which may undergo internalization. Methyl-β-cyclodextrin (MCD) treatment greatly reduced cholesterol and shifted DOR to higher density fractions and decreased DPDPE affinities. MCD treatment attenuated DPDPE-induced $[^{35}S]$GTPγS binding in CPu and NG108-15 cells, but enhanced it in CHO-FLAG-mDOR cells. In CHO-FLAG-mDOR cells, $G_{αi}$ co-immuno-precipitated with caveolin-1, which was shown to inhibit $G_{αi/o}$, and MCD treatment drama-tically reduced the association leading to disinhibition. Thus, although localization in rafts and agonist-induced shift of DOR are independent of caveolin-1, lipid rafts sustain DOR-mediated signaling in caveolin-deficient neuronal cells, but appear to inhibit it in caveolin-enriched non-neuronal cells. Cholesterol-dependent association of caveolin-1 with and the resulting inhibition of G proteins may be a contributing factor.

* Corresponding author. Tel.: +1 215 707 4188; fax: +1 215 707 7068.
  E-mail address: lliuche@temple.edu (L.-Y. Liu-Chen).
  Abbreviations: CPu, caudate putamen; CHO cells, Chinese hamster ovary cells; CHO-FLAG-mDOR, CHO cells stably transfected with FLAG-mDOR cDNA; DPDPE, [D-Pen^2,D-Pen^5]-Enkephalin; DTT, dithiothreitol; FLAG epitope, (DYKDDDDK); FLAG-mDOR, FLAG-tagged mouse δ opioid receptor; GM1, ganglioside M1; GPCRs, G protein-coupled receptors; HRP, horseradish peroxidase; MCD, methyl-β-cyclodextrin; MES, 2-morpholinoethanesulfonic acid; PMSF, phenylmethylsulfonyl fluoride; SDS-PAGE, sodium dodecyl sulfate-poly-acrylamide gel electrophoresis; TBS-T, 10 mM Tris–HCl, 159 mM NaCl, 0.1% Tween-20, pH 7.4

1. Introduction

At least three types of opioid receptors (μ, δ and κ) mediate pharmacological effects of opioid drugs and physiological actions of endogenous opioid peptides. The δ opioid receptor (DOR) has been associated with analgesia, morphine tolerance and mood regulation [1,2]. The δ opioid agonists may potentially be used as analgesics with less side effects associated with the μ agonists as well as anxiolytics and antidepressants [2,3]. The DOR is mainly distributed in neurons, and is also found in non-neuronal cells, including the rat and human heart myocytes [4,5]. In the heart, activation of DOR produces negative ionotropic effects and δ agonists have cardio-protective effects [6,7]. Opioid receptors are members of the rhodopsin sub-family of G protein-coupled receptors (GPCRs) and are coupled primarily to G_i/G_o proteins to modulate several downstream effectors, including inhibition of adenylyl cyclases, enhancement of K^+ conductance, attenuation in Ca^{2+} conductance and stimulation of p42/p44 mitogen-activated protein (MAP) kinases (for a review, see [8]).

Lipid rafts are small, low-density, cell plasma membrane domains enriched in cholesterol and glycosphingolipids (e.g., GM1) in the outer layer. Recently, it was proposed that they should be termed "membrane rafts", as it has become increasingly apparent that proteins play a major role in their formation and contribute to their function [9]. Thus, the term membrane rafts and lipid rafts will be used interchangeably. Since Brown and Rose [10] gave the operation definition of lipid rafts, the concept has been developed largely based on their biochemical nature of insolubility in non-ionic detergents at low temperature and high buoyancy in density gradients. Lipid rafts are classified into planar lipid rafts and caveolae. Morphological identification of planar lipid rafts has been elusive [11]. One the contrary, electron micrographs show that caveolae are flask-shaped membrane invaginations at plasma membranes in most differentiated cells [12]. Caveolins, three structural and scaffolding proteins, form a cytoplasmic coat on the invaginated structures and appear to stabilize the identifiable shape of caveolae [13].

Of particular interest has been the notion that lipid rafts act as organizational platforms for signal transduction, as a variety of membrane proteins involved in signaling were found to be enriched in or recruited into lipid rafts/caveolae [12,14,15]. Caveolins have been reported to interact with and concentrate many signaling proteins within caveolae, and, in most cases, negatively regulate their activities [12,16]. A number of GPCRs and their downstream effectors, such as G_α proteins, protein kinase C and adenylyl cyclases, have been demonstrated to be regulated by lipid rafts/caveolae [14,15,17].

Investigations on effects of lipids on binding properties and signaling of opioid receptors could be traced back to 1980s. For examples, incorporation of cerebroside sulfate (a glycosphingolipid) or phosphatidylcholine augments both the potencies and the efficacies of morphine and enkephalin to regulate adenylyl cyclase activity in N18TG2 cells without changing the number of the DOR binding sites [18]. Increasing membrane cholesterol in N1E-115 neuroblastoma cells reduced [3H]met-enkephalin binding activity at DOR [19]. Lipids were required for the binding activity of partially purified μ opioid receptors and specificity of the requirement was defined [20].

Opioid receptors, like many other GPCRs, have been recently shown to locate in lipid rafts/caveolae in caveolin-rich non-neuronal cells, and such localization plays important roles in receptor functions, including the κ opioid receptors expressed in CHO cells [21], the μ opioid receptors transfected into HEK293 cells [22] and μ and δ opioid receptors in adult rat cardiac myocytes [23,24]. The μ, δ and κ opioid receptors have caveolin-1-binding consensus sequences (the "ϕXϕXXXXϕ motif", where ϕ is an aromatic residue [25]), "YAFLDENF", at the junction of TMs7 and C-tails. We have found that caveolin-1 co-immunoprecipitated with FLAG-tagged human κ opioid receptors expressed in CHO cells [21].

Neurons in the brain had been demonstrated to be deficient in caveolin-1 and devoid of caveolae [26]. Although numerous GPCRs are present in neurons in the brain, whether GPCRs, including opioid receptors, are localized in low-density cholesterol- and glycosphingolipids-rich membrane domains (non-caveolae lipid rafts) remains unclear. In addition, little is known about the role of the non-caveolae lipid rafts in regulating GPCRs in neuronal cells or tissues.

In this study, we found the opioid receptors in the rat caudate putamen (CPu), the δ opioid receptor (DOR) endogenously expressed in NG108-15 neuroblastoma x glioma hybrid cell line and FLAG-mouse-DOR expressed in CHO cells (CHO-FLAG-mDOR) were localized in lipid rafts. NG108-15 cells have long been used as an *in vitro* neuron-like model to study opioid receptor properties and signaling. We observed that NG108-15 cells had no detectable caveolin-1 and the rat brain expressed a very low level of caveolin-1, whereas there was abundant caveolin-1 in CHO cells. We examined and compared the role of lipid rafts in opioid receptor functions in the three systems and delineated possible mechanisms underlying the differences.

2. Materials and methods

2.1. Materials

[3H]diprenorphine (58 Ci/mmole) and [35S]guanosine 5-(γ-thio)triphosphate (GTPγS) (1250 Ci/mmole) were purchased from Perkin-Elmer Co. (Boston, MA). Naloxone was a gift from the former DuPont/Merck Co. (Wilmington, DE). DPDPE, deltorphin II and etorphine were provided by Drug Supply System of National Institute on Drug Abuse (NIDA). Sodium carbonate, 2-morpholinoethanesulfonic acid (MES), glycerol, ethylenediamine tetraacetic acid (EDTA), ethylene glycol-bis(β-aminoethyl ether)-N,N,N',N'-tetraacetic acid (EGTA), dithiothreitol (DTT), PMSF, GDP, GTPγS, methyl-β-cyclodextrin (MCD), HAT and anti-FLAG monoclonal antibody (M1) were purchased from Sigma Co. (St Louis, MO). For phosphate assay, hydrogen peroxide, Fisk-Subbarrow reducer and phosphate standard were obtained from Sigma (St Louis, MO) and ammonium molybdate was purchased from Fisher (Newark, DE). Ammonium persulfate was purchased from Bio-Rad Laboratories (Hercules, CA). Anti-GM1 polyclonal antibody was purchased from Calbiochem (San Diego, CA). Anti-caveolin-1 monoclonal antibody (clone 2297) and anti-flotillin-1 monoclonal antibody were obtained from BD Transduction Laboratories (San Jose, CA). Polyclonal anti-$G_{\alpha i3}$ antibody,

which recognizes $G_{\alpha i1}$, $G_{\alpha i2}$ and $G_{\alpha i3}$, and Protein A/G PLUS-Agarose were obtained from Santa Cruz Biotechnology (Santa Cruz, CA) and Immobilon-P transfer membrane from Millipore Corporation (Billerica, MA). Goat anti-mouse IgG conjugated with horseradish peroxidase (HRP) was from Jackson ImmunoResearch Laboratories Inc. (West Grove, PA). Goat anti-rabbit IgG conjugated with HRP, SuperSignal West Pico Chemiluminescent Substrate Solution and Restore™ Western Blot Stripping Buffer were from Pierce Co. (Rockford, IL). Mini Complete™ Protease Inhibitor Cocktail was from Roche (Nutley, NJ).

2.2. Cell lines

NG108-15 mouse neuroblastoma $\times$ rat glioma hybrid cells, which express $\sim$0.6 pmole δ opioid receptors/mg membrane protein, were cultured in a humidified 5% (v/v) CO_2/air incubator at 37 °C in Dulbecco's modified Eagle's medium/HAT (0.1 mM hypoxanthine, 10 μM aminopterin and 17 μM thymidine)/10% fetal bovine serum/100 U/ml penicillin and 100 μg/ml streptomycin. Clonal CHO cell lines stably expressing FLAG-mDOR were established as described previously [27]. CHO-FLAG-mDOR cells were cultured in Dulbecco's modified Eagle's medium F12 HAM supplemented with 10% fetal calf serum, 0.1 mg/ml geneticin, 100 U/ml penicillin and 100 μg/ml streptomycin in a humidified atmosphere consisting of 5% CO_2 and 95% air at 37 °C.

2.3. Rat brain CPu membrane preparation

The frozen meninges-stripped rat brains were purchased from Pel-Freeze Biologicals (Rogers, AR). The caudate putamen tissues were dissected and homogenized in $\sim$8 vol. 10 mM TEL buffer (10 mM Tris, 1 mM EGTA, 0.32 M sucrose, 10 mM glucose and 10 μM leupeptin, pH 7.4). After centrifugation at $\sim$920 $\times$ g for 10 min, the supernatant was saved and centrifuged again at $\sim$100,000 $\times$ g for 20 min. The pellet was resuspended in 5 mM TEL buffer (5 mM Tris, 5 mM EDTA, 5 mM EGTA and 10 μM leupeptin, pH 7.4) and stayed on ice for 30 min. After homogenization to disrupt synaptosomes, the homogenate was centrifuged at $\sim$100,000 $\times$ g for 30 min. The brown tight pellet at bottom was discarded and the top layer of loose pellet was saved for lipid rafts isolation as below. All procedures were performed at 4 °C or on ice.

Detergent-free preparation of lipid rafts using sodium carbonate were conducted according to Song et al. [28] with some modifications (Fig. S1). One notable modification is the use of 8 ml of 5–35% continuous sucrose gradient on top of 4 ml of 45% sucrose in centrifugation, instead of 5%/35%/45% discontinuous gradient, to facilitate detection of receptor shift following treatment with an agonist or MCD [21]. Cells were grown to confluence in 100-mm tissue culture plates, harvested, and centrifuged at 300 $\times$ g for 5 min. Cell pellets or rat brain CPu membranes were resuspended in 2 ml of 500 mM sodium carbonate buffer (pH 11), and homogenized using a Thomas loose fitting Teflon homogenizer (10 strokes) followed by sonication (three or eight 20-s bursts at 6 W) on ice using a Fisher Sonic Dismembrator 60. Two milliliters of 90% sucrose prepared in MES-buffered saline (MBS) (20% glycerol, 150 mM NaCl, 2 mM EDTA, 25 mM MES, pH 6.5) were added to the homogenized samples yielding 45% sucrose in a total volume of 4 ml. An 8-ml continuous gradient of 5–35% sucrose prepared in MBS buffer containing 0.25 M sodium carbonate (for discontinuous gradient, 4 ml of 5% sucrose and 4 ml of 35% sucrose) was layered on the top of the 45% fraction. Isopycnic ultracentrifugation were then carried out at 39,000 rpm ($\sim$190,000 $\times$ g) using a Beckman ultracentrifuge and a SW 41 rotor for 16–20 h at 4 °C. Following ultracentrifugation, twelve 1 ml fractions were collected from the bottom of the gradient tube using a peristaltic pump.

2.4. Determination of cholesterol and phopholipid contents

Lipid raft fractions or cells were extracted by a chloroform: methanol solvent mixture (2:1, v/v). Cholesterol content in the chloroform layer was taken out for cholesterol and phospholipid determinations. The amount of cholesterol was determined using a cholesterol reagent (Cholesterol E) obtained from Waco Chemicals USA (Richmond, VA). The phospholipid concentrations in cell membranes were determined by the method of [29]. The cholesterol content in the raft fractions was expressed as the ratios of cholesterol in each fraction relative to total phospholipids.

2.5. Analysis of GM1 ganglioside

GM1 level in each fraction of rat brain CPu membranes or NG108-15 cells was determined by a dot-blot assay using an anti-GM1 antibody (Calbiochem), which does not cross react with other carbohydrate epitopes. Briefly, 1.0 μl of each sucrose gradient fraction sample (CPu fraction samples were all 1:10 diluted) was spotted onto a nitrocellulose membrane (Invitrogen), air-dried for 30 min, and washed with TBS for three times. Membranes were blocked with 3% (w/v) BSA in TBS, and incubated with anti-GM1 (1:1000) at 4 °C over night. Blots were washed and incubated with HRP-conjugated anti-rabbit IgG at 4 °C for 1 h. Spots were visualized by chemiluminescence using Pierce SuperSignal kit according to the manufacturer's instructions, and the signals were captured via the Fujifilm LAS1000 plus imaging system.

Immunoblotting of FLAG-mDOR, caveolin-1 and flotillin-1 were carried out according to our published method [21,30], using monoclonal antibodies against the FLAG-tag (M1), caveolin-1 (clone 2297) and flotillin-1, respectively.

2.6. Reduction of cell membrane cholesterol content by 2% of methyl-β-cyclodextrin (MCD) treatment

For NG108-15 cells or CHO-FLAG-mDOR cells, cells were incubated with MCD for 1 h at 37 °C in the serum-free medium, while control cells received serum-free medium alone. Following incubation, MCD was removed by washing three times in cold PBS. For rat brain CPu, brain membranes (2 mg of protein) were prepared as above and then suspended in 20 ml of 5 mM TEL buffer with or without 2% MCD and incubated at 37 °C for 1 h. The membranes were then centrifuged at $\sim$100,000 $\times$ g at 4 °C for 30 min. The pelleted membranes were washed twice by suspension in the 20 ml TEL buffer and centrifugation at $\sim$100,000 $\times$ g at 4 °C for 30 min.

2.7. [^{35}S]GTPγS binding

Determination of [^{35}S]GTPγS binding to G proteins was carried out using a modified procedure of Zhu et al. [31]. CHO-FLAG-mDOR cells, NG108-15 cells were incubated with vehicle or 2% MCD as described and harvested, and membranes were prepared as described previously. Rat brain CPu membranes were treated with MCD as described above. Membranes (10 μg protein) were incubated in reaction buffer (50 mM HEPES, 100 mM NaCl, 5 mM MgCl$_2$, 1 mM EDTA) containing [^{35}S]GTPγS (100,000–150,000 dpm, 80–100 pM) and GDP (10 μM for CHO-FLAG-mDOR cells; 80 μM for NG108-15 cells and rat brain CPu) with or without DPDPE (10^{-10} to 10^{-5} M) in a total volume of 0.5 ml for 60 min at 30 °C. Nonspecific binding was determined in the presence of 10 μM GTPγS. Bound and free [^{35}S]GTPγS were separated by filtration with GF/B filters under reduced pressure. Radioactivity was determined by liquid scintillation counting with a counting efficiency of 95%.

2.8. Ligand binding to opioid receptors

Binding was performed on each fraction of rat brain CPu membranes, NG108-15 cells or CHO-FLAG-mDOR preparations after sucrose gradient centrifugation with [^{3}H]diprenorphine (1 nM) in 50 mM Tris–HCl buffer/1 mM EGTA (pH7.4) (TE buffer) at room temperature for 1 h in duplicate according to our published procedure [32]. Nonspecific binding was defined as binding in the presence of naloxone (10 μM).

Saturation binding of [^{3}H]diprenorphine to δ opioid receptors in membranes of NG108-15 cells or CHO-FLAG-mDOR cells treated with or without 2% MCD was performed with at least six concentrations of [^{3}H]diprenorphine (ranging from 25 pM to 2 nM), and K_d and B_{max} values were determined [33]. Competition inhibition by DPDPE of [^{3}H]diprenorphine (0.5 nM) binding to δ opioid receptors was performed in the absence or presence of various concentrations of DPDPE and its K_i value was determined [31].

2.9. Co-immunoprecipitation of G$_{\alpha i}$ proteins and caveolin-1

CHO-FLAG-mDOR cells (3×10^6) were incubated with vehicle or 2% MCD as described, harvested, and then solubilized in the solubilization buffer (50 mM Tris–HCl, 150 mM NaCl, 1 mM EDTA, Roche mini Complete^{TM} Protease inhibitors at 1 pill/10 ml and 2% Triton X-100) at 4 °C for 1 h and centrifuged at 100,000 × g, 4 °C for 30 min. Supernatants were collected and incubated with or without 10 μl (2 μg) of rabbit anti-G$_{\alpha i-3}$ at 4 °C for 1 h, and then 20 μl of resuspended Protein A/G PLUS-Agarose for 1 h at 4 °C on a rocker platform. The agarose pellets were collected, washed with 1.0 ml of TBS-T for four times, and resuspended in 40 μl of 2× Laemmli sample buffer. Twenty microliters of each samples were separated on SDS-PAGE and caveolin-1 was detected using a monoclonal anti-caveolin-1 (1:1000) as described above. Membranes were then stripped and G$_{\alpha i}$ proteins on the membranes were detected with immunoblotting using rabbit anti-G$_{\alpha i-3}$ (1:250), followed by goat anti-rabbit IgG conjugated with HRP and chemiluminescence reagents. Anti-G$_{\alpha i-3}$ recognizes G$_{\alpha i-1}$, G$_{\alpha i-2}$ and G$_{\alpha i-3}$.

3. Results

3.1. Differential expression of caveolin-1 in CHO cells versus rat brain and NG108-15 cells

Expression of caveolin-1 and flotillin-1 were examined by immunoblotting. Flotillin-1 was shown to be expressed at comparable levels in the two cell lines and rat brain. However, caveolin-1 was abundant in CHO-FLAG-mDOR cells, but very low in the rat brain and undetectable in NG108-15 cells (Fig. 1).

3.2. Opioid receptors in rat brain CPu and DOR in NG108-15 cells and CHO cells are localized in lipid rafts

The rat brain caudate putamen (CPu) has a relatively high level of opioid receptors, which are present in neurons [34]. To prepare lipid raft, we used a modified version of our published procedure [21], which was based on the detergent-free method of Song et al. [28]. It should be noted that this method does not distinguish between planar lipid rafts and caveolae. The term "lipid rafts" or "membrane rafts" will be used in this paper.

CPu membranes, NG108-15 cells and CHO-FLAG-mDOR cells were sonicated in a 500 mM sodium carbonate buffer (pH 11) on ice, and as shown in Fig. S1, the mixture was fractionated in a 5%/35%/45% discontinuous sucrose density gradient by ultracentrifugation, and twelve 1 ml fractions were collected. A light-scattering band appeared in the low-density region at the junction of 5% and 35% sucrose, i.e. fractions 4 or 5.

For CPu (Fig. 2), cholesterol and flotillin-1 levels peaked in fraction 5, which was at the interface of 5%/35% sucrose in the gradient (Fig. 2A and B), so did the opioid receptor binding (Fig. 2C). The low-density fractions (1–5) at 5%/35% interface and above contained 77.0% of total cholesterol (Fig. 2A), significantly higher level of flotillin-1, and 82.7% of total opioid receptor binding sites (Fig. 2C). For NG108-15 cells (Fig. 3A) and CHO-FLAG-mDOR cells (Fig. 3B), in a similar manner, DOR binding (Fig. 3A and B, upper panels) and cholesterol (data not shown) consistently peaked in fractions at the interface of 5%/35% sucrose gradients, which was fractions 5 and 4, respectively,
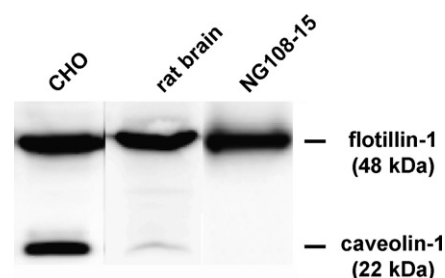

Fig. 1 – Immunoblotting of caveolin-1 and flotillin-1 in CHO cells, rat brains and NG108-15 cells. Cells or tissues were homogenized in TE buffer (pH7.4) including protease inhibitors, boiled in 1× Lammli loading buffer, and resolved on 12% SDS-PAGE. Immunoblotting was performed with monoclonal antibodies against flotillin-1 and caveolin-1, respectively. Twenty mirograms of proteins per lane were loaded. The figures represent one of the three experiments performed with similar results.
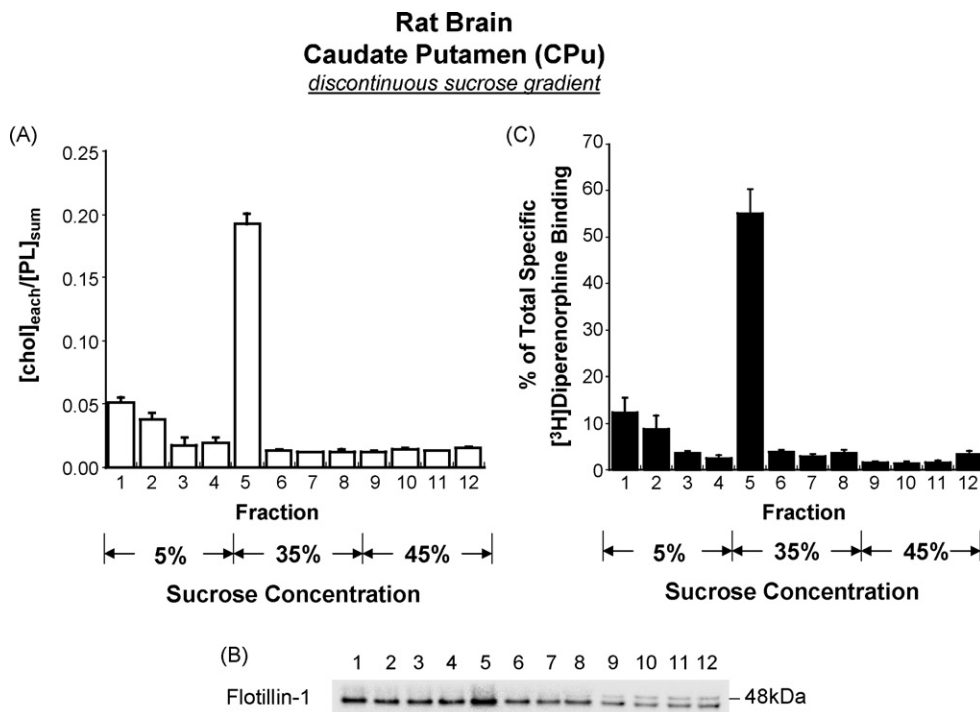
Fig. 2 – Localization in lipid rafts of opioid receptors in membranes of the rat caudate putamen (CPu). CPu membranes prepared from six rats were sonicated in 0.5 M sodium carbonate buffer (pH 11) and then fractionated through a discontinuous sucrose gradient (5%/35%/45%) by ultracentrifugation as described under Section 2 (see Fig. S1). Twelve 1-ml fractions were collected and each fraction was subjected to (A) determination of cholesterol contents. Data are expressed as the ratios of (cholesterol in each fraction)/(total phospholipids). (B) Flotillin-1 immunoblotting with an anti-flotillin-1 monoclonal antibody. (C) [³H]diprenorphine (~1 nM) binding using naloxone (10 μM) to define nonspecific binding. Two 100-μl aliquots from each fraction were used in binding in duplicate as described in Section 2. Data are expressed as % of total specific [³H]diprenorphine binding. Data are shown as mean ± S.E.M. of three independent experiments.

due to slight variations in fraction collection. In both cell lines, the low-density fractions similarly contained most of DOR binding sites (Fig. 3A and B, upper panels) and cholesterol contents (data not shown). Thus, a majority of opioid receptors in the rat CPu and DOR in both caveolin-deficient neuronal cells and caveolin-rich non-neuronal cells located in buoyant cholesterol-rich membrane domains, namely membrane rafts.

In addition to receptor binding, we detected FLAG-mDOR in each fraction derived from CHO-FLAG-mDOR cells by immunoblotting with anti-FLAG antibody and found that the distribution of FLAG-mDOR immunoreactivity was similar to that of receptor binding (Fig. 3B, middle panel). Besides cholesterol, the distributions of two other lipid rafts markers, flotillin and caveolin-1, correlated well with the DOR localization, further validating the results. In NG108-15 cells, flotillin-1 peaked at fraction 5 and located mostly among low-density fractions (Fig. 3A, lower panel). In CHO-FLAG-mDOR cells, caveolin-1 and flotillin-1 peaked at fraction 4 and distributed predominantly in low-density fractions (Fig. 3B, two lower panels). In contrast, the majority of proteins were in higher density fractions, particularly fractions 10–12 (data not shown). In addition, ganglioside M1 (GM1), a glycosphingolipid rafts marker, was also found mainly in low-density fractions in the following experiments using continuous sucrose gradient to isolate lipid rafts (see Fig. 4C).

3.3. Fractionation by continuous sucrose density gradient centrifugation to isolate lipid rafts

In order to facilitate detection of receptor shift following treatment with a ligand or MCD, fractionation through continuous sucrose density gradient (5–35%/45%), instead of discontinuous one (5%/35%/45%) (both shown in Fig. S1), was used in the following experiments.

For rat brain CPu membranes, following continuous sucrose gradient centrifugation, cholesterol levels and GM1 immunoreactivities peaked in fraction 1 (Fig. S2A, S2B), so did opioid receptors (Fig. S2C). Since low-density and high levels of cholesterol and glycosphingolipids, such as GM1, are characteristics of membrane rafts microdomains [16], these results validated the membrane rafts preparation method we used. More importantly, the raft fractions were narrowed down to fractions 1–4, corresponding to a concentration range of 5% to ~20% sucrose, similar in density to the membrane rafts isolated through continuous-density gradients by Brown and Rose [10] and Macdonald and Pike [35] using detergent- and non-detergent methods, respectively. The raft fractions (1–4) contained 63.9% of total cholesterol (Fig. S2A), the overwhelming majority of GM1 (Fig. S2B) and 69.4% of total opioid receptor [³H]diprenorphine binding (Fig. S2C). It is noteworthy that the raft fractions (1–4) contain only
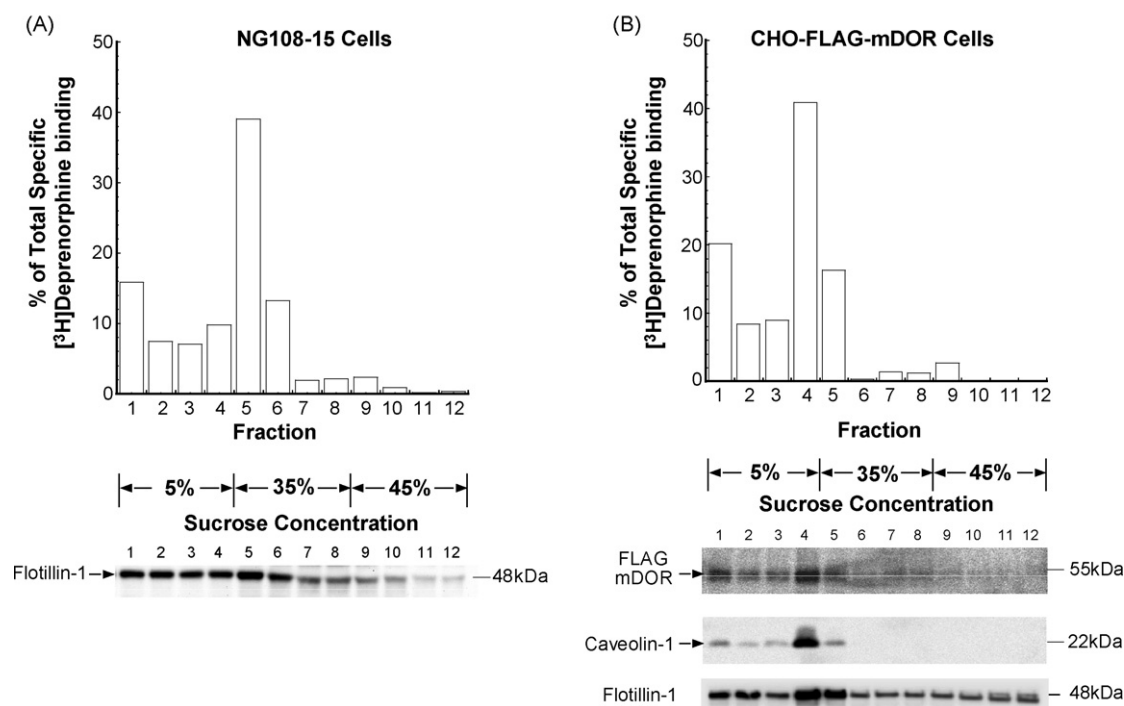
discontinuous sucrose gradient

Fig. 3 – Localization in lipid rafts of DOR in NG108-15 cells and CHO cells. Lipid rafts were isolated by discontinuous sucrose gradients in a similar manner as in Fig. 2. Twelve 1-ml fractions were collected and each fraction was subjected to [³H]diprenorphine (∼1 nM) binding and Western blot assays, respectively. (A) NG108-15 cells: upper panel is for [³H]diprenorphine (∼1 nM) binding, lower panel is for immunoblotting by a monoclonal anti-flotillin-1 antibody. (B) CHO-FLAG-mDOR cells: upper panel is for [³H]diprenorphine (∼1 nM) binding, middle panel is for immunoblotting by a monoclonal anti-FLAG antibody M1, and the two lower panels are for immunoblotting by monoclonal anti-caveolin-1 and anti-flotillin-1 antibodies, respectively.

small portion of total membrane proteins, while the high-density fractions 9–12 contain most membrane proteins (Fig. S2D).

NG108-15 cells were also subjected to lipid rafts preparation procedure with the same fractionation through continuous sucrose gradients. The highest level ($28.8 \pm 0.6\%$, $n = 3$) of [³H]diprenorphine binding was detected in fraction 1 (Fig. 4A, control), coincided with the peaks of cholesterol (Fig. 4B, control) and GM1 (Fig. 4C, control). A majority (66.8%) of DOR binding activity was found in low-density raft fractions 1–4 (Fig. 4A, control).

Similar procedures and fractionation were carried out on CHO-FLAG-mDOR cells. As determined by [³H]diprenorphine binding, DOR was localized primarily in low-density fractions with 70.1% of total binding activity in fractions 1–4 (Fig. 5A control). Immunoblotting with anti-FLAG antibody also revealed that raft fractions 1–4 contained the bulk of FLAG-mDOR (Fig. 5B control). In contrast, the bottom fractions 9–12 had highest protein contents (data not shown).

In summary, fractionation through continuous gradients gave a better resolution and revealed that 66–70% of opioid receptors in rat brain CPu membranes as well as DOR in NG108-15 cells and CHO cells are localized in lipid rafts—fractions 1–4% with a 5–20% sucrose density.

3.4. Acute treatment with full agonists moved some DOR out of lipid rafts in NG108-15 and CHO cells in a similar manner

To study agonist effect on localization of DOR in lipid rafts, we treated NG108-15 cells for 30 min at 37 °C with vehicle or a full agonist and then isolated rafts through continuous sucrose gradients. Etorphine treatment greatly decreased [³H]diprenorphine binding in fractions 1 and 2 (both $P < 0.001$, $n = 3$) (Fig. 4A). In contrast, etorphine significantly increased [³H]diprenorphine binding in fractions 5, 9 and 11 (all $P < 0.05$, $n = 3$) (Fig. 4A). About 67% of total DOR was found in low-density raft fractions 1–4 in control cells (Fig. 4A, control). Etorphine treatment moved ∼28% of rafts DOR out of lipid rafts and shifted them to high-density non-rafts fractions (Fig. 4A, etorphine). However, etorphine treatment did not significantly change the distributions of the lipid rafts markers cholesterol (Fig. 4B) and GM1 (Fig. 4C) among the 12 fractions. Treatment with DPDPE or deltorphin II at 1 μM similarly decreased the binding activities in fractions 1 and 2 and increased those in fractions 5, 9 and 11, compared with control cells (Fig. S3A). In contrast to the full agonists, neither the partial agonist levorphanol (1 μM) nor the antagonists/inverse agonists naloxone (10 μM) and ICI174,864 (1 μM) induced any
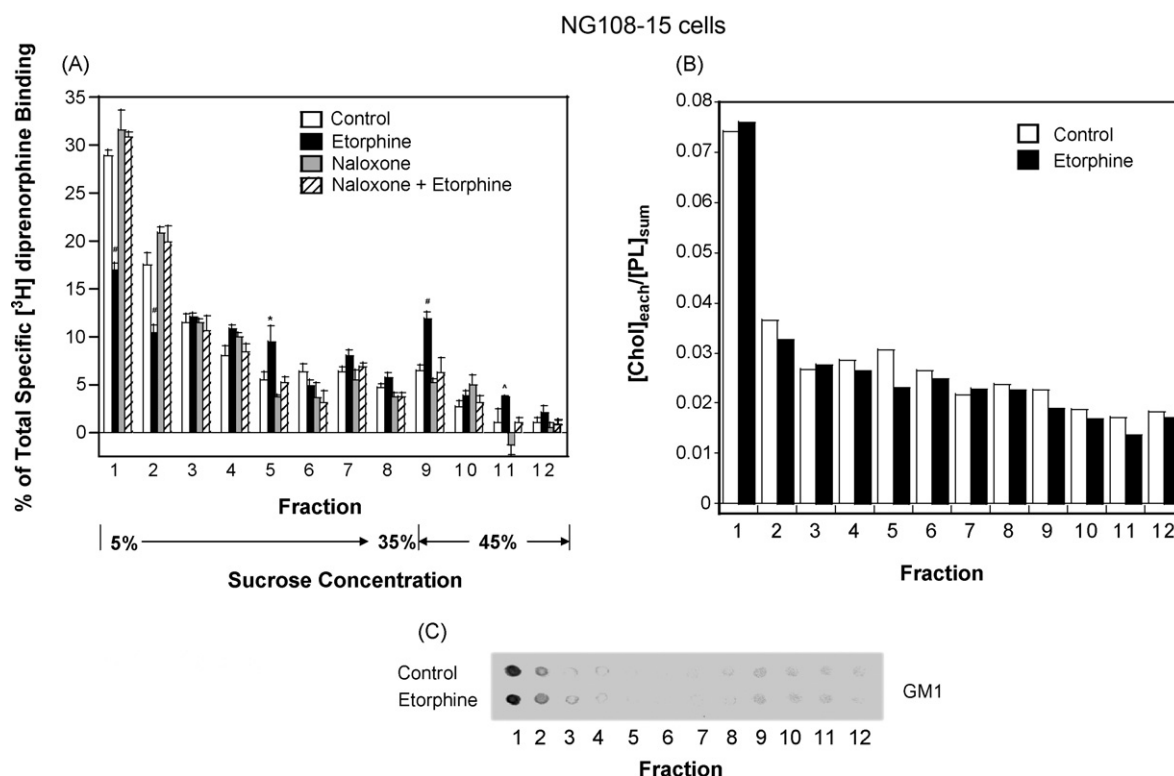
Fig. 4 – Agonist treatment affected DOR localization in lipid rafts in NG108-15 cells. (A) Effect of etorphine to shift DOR out of lipid rafts was blocked by naloxone. (B) Determination of cholesterol contents. Data are expressed as the ratios of (cholesterol in each fraction)/(total phospholipids). (C) Determination of GM1 levels by a dot-blot assay with an anti-GM1antibody. Cells were left untreated or incubated in the media in the presence of 1 μM etorphine, 10 μM naloxone or both for 30 min at 37 °C; after various treatments, ten 100-mm dishes of confluent NG108-15 cells were scraped off the plates and collected. Fractionation to isolate lipid rafts through continuous sucrose gradients was performed, 12 fractions were collected and each fraction was subjected to [^{3}H]diprenorphine ($\sim$1 nM) binding as described in Fig. 2 legend. The average [^{3}H]diprenorphine-specific binding in the fraction 1 was 1758 dpm/100 μl. Data in A are shown as mean $\pm$ S.E.M. of three independent experiments. B or C represents one of the two experiments performed with similar results. [#]P < 0.001, [*]P < 0.01, [^]P < 0.05, by one-way ANOVA followed by Tukey's multiple comparisons test.

significant changes in distribution of DOR in lipid rafts in NG108-15 cells (see naloxone data in Fig. 4A; other data in Fig. S3B). Levorphanol was a partial agonist in [^{35}S]GTPγS binding with $\sim$40% of the efficacy of DPDPE (data not shown). Similarly, 10 μM morphine, a partial agonist, did not cause any shift (Fig. S3B). The results indicate that shifting DOR out of lipid rafts is dependent on efficacy of the ligand.

Etorphine effect was also determined in CHO-FLAG-mDOR cells in a similar manner. In control cells, 70.1% of total [^{3}H]diprenorphine binding to DOR (Fig. 5A control) and the majority of FLAG immunoreactivity (Fig. 5B control) were localized in low-density rafts fractions 1–4. A 30-min etorphine treatment moved $\sim$23% of rafts FLAG-mDOR out of lipid rafts. DOR, as determined by [^{3}H]diprenorphine binding, in fractions 1 and 2 were substantially decreased (both P < 0.001, n = 3), while those in fractions 7–9 were significantly increased (all P < 0.001, n = 3) (Fig. 3A). Western blot data displayed a similar trend of shift of the DOR protein out of low-density fractions 1–3 to high-density fractions 5–9 (Fig. 5B). In contrast, etorphine treatment did not significantly change the distribution of caveolin-1 (Fig. 5C) and cholesterol (Fig. 5D). Thus, acute

treatment with a full agonist moves DOR out of lipid rafts in CHO cells in a similar manner as in NG108-15 cells.

3.5. Agonist-induced shift of DOR out of lipid rafts is naloxone-reversible and PTX-insensitive

When NG108-15 cells were incubated with 10 μM of naloxone for 5 min and then 1 μM of etorphine was added for another 30 min at 37 °C, DOR was not moved out of lipid rafts fractions, indicating that etorphine-induced DOR movement is mediated by receptor activation (Fig. 4A).

Incubation of NG108-15 cells with 100 ng/ml of PTX for 24 h did not change DOR distribution in NG108-15 cells, nor did it affect etorphine-induced shift of DOR out of lipid rafts (Fig. S4) although it totally abolished etorphine-stimulated [^{35}S]GTPγS binding to membranes (data not shown). These results from NG108-15 cells indicate that (1) localization of DOR in lipid rafts is independent of the receptor coupling to $G_{i/o}$ protein, and (2) activation of the receptor, but not $G_{i/o}$ proteins, is necessary for agonist-induced shift of DOR out of lipid rafts.
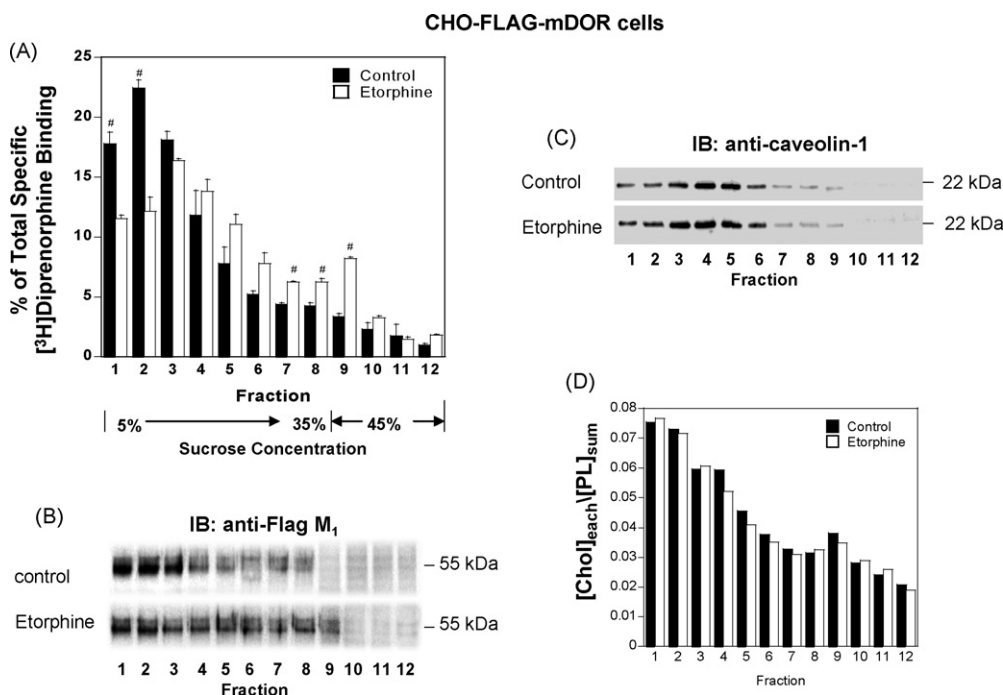
Fig. 5 – FLAG-DOR expressed in CHO cells was shifted out of lipid rafts by etorphine treatment. CHO-FLAG-mDOR cells were incubated at 37 °C in the absence and presence of 1 μM etorphine for 30 min. Cells were collected and fractionation for lipid rafts was performed. Twelve fractions from continuous sucrose gradients were collected and each fraction was subjected to (A) [³H]diprenorphine (∼1 nM) binding and data were expressed as % of total specific [³H]diprenorphine binding. Three 100-mm dishes of confluent CHO-FLAG-mDOR cells were used for fractionation and two 100 μl-aliquots of each 1-ml fraction were used in binding in duplicate. The average [³H]diprenorphine-specific binding in the fraction 1 was 9212 dpm/100 μl. Data are shown as mean ± S.E.M. from three independent experiments. #P < 0.001, by one-way ANOVA followed by Tukey's multiple comparisons test. (B) Immunoblotting of FLAG-DOR with an anti-FLAG monoclonal antibody M₁. (C) Caveolin-1 immunoblotting with an anti-caveolin-1 monoclonal antibody. (D) Determination of cholesterol contents. Data are expressed as the ratios of (cholesterol in each fraction)/(total phospholipids). Fig. 5B, C or D represents one of the two experiments performed with similar results.

3.6. Methyl-β-cyclodextrin (MCD) treatment greatly reduced cholesterol contents and shifted the DOR in cells and opioid receptors in rat CPu to fractions of higher density

MCD removes cholesterol from plasma membranes of cultured cells [36], resulting in reduction or disruption of lipid rafts [37]. Pre-treatment with 2% MCD for 1 h at 37 °C caused 52.0 ± 3.9%, 49.6 ± 3.4% and 76.7 ± 1.2% reduction in cholesterol content in NG108-15 cells, CHO-FLAG-mDOR cells and rat CPu membranes, respectively.

To examine whether the buoyancy of receptors in rafts is sustained by cholesterol, we carried out the same continuous sucrose density fractionation for the cells/tissues after cholesterol depletion with MCD (Fig. 6).

Compared with the control, MCD treatment of NG108-15 cells reduced cholesterol levels in all 12 fractions and eliminated any significant peak with the greatest reduction in fraction 1 (Fig. 6A). In addition, high levels of [³H]diprenorphine binding were shifted by MCD treatment from fraction 1 to higher density fractions, with the peaks in the fractions 4–6 (Fig. 6B).

Following MCD treatment, cholesterol levels in CHO-FLAG-mDOR cells were reduced in all 12 fractions, with no significant peak, and the lower the fraction density was, the greater the reduction was, compared with the control cells (Fig. 6C). High levels of [³H]diprenorphine binding was shifted from fractions 1–4 to 4–8 (Fig. 6D) and high contents of caveolin-1 were shifted from fractions 1–6 to higher density fractions 3–9 (Fig. 6E).

For control CPu membrane, about 50% of cholesterol and [³H]diprenorphine bindings were detected in fractions 1 (Fig. 6F and G). MCD treatment reduced cholesterol contents in CPu membranes to a greater extent than in the two cell lines, with a higher level of depletion in low-density fractions and only a small peak left in fraction 1 (Fig. 6F). Concomitantly, [³H]diprenorphine binding was shifted out of fractions 1–3 to 4–10, with only a small peak left in fraction 1 (Fig. 6G).

Collectively, these results demonstrated that in different tissues/cells, MCD treatment reduced cholesterol, leading to disruption of lipid rafts and shift of the receptor to high-density fractions. Thus, the high cholesterol contents in lipid rafts are necessary to sustain the buoyancy of opioid receptors.

3.7. Effects of MCD treatment on DOR ligand binding

As shown in Table 1, in both CHO-FLAG-mDOR cells and NG108-15 cells, incubation with 2% MCD increased both the K_i
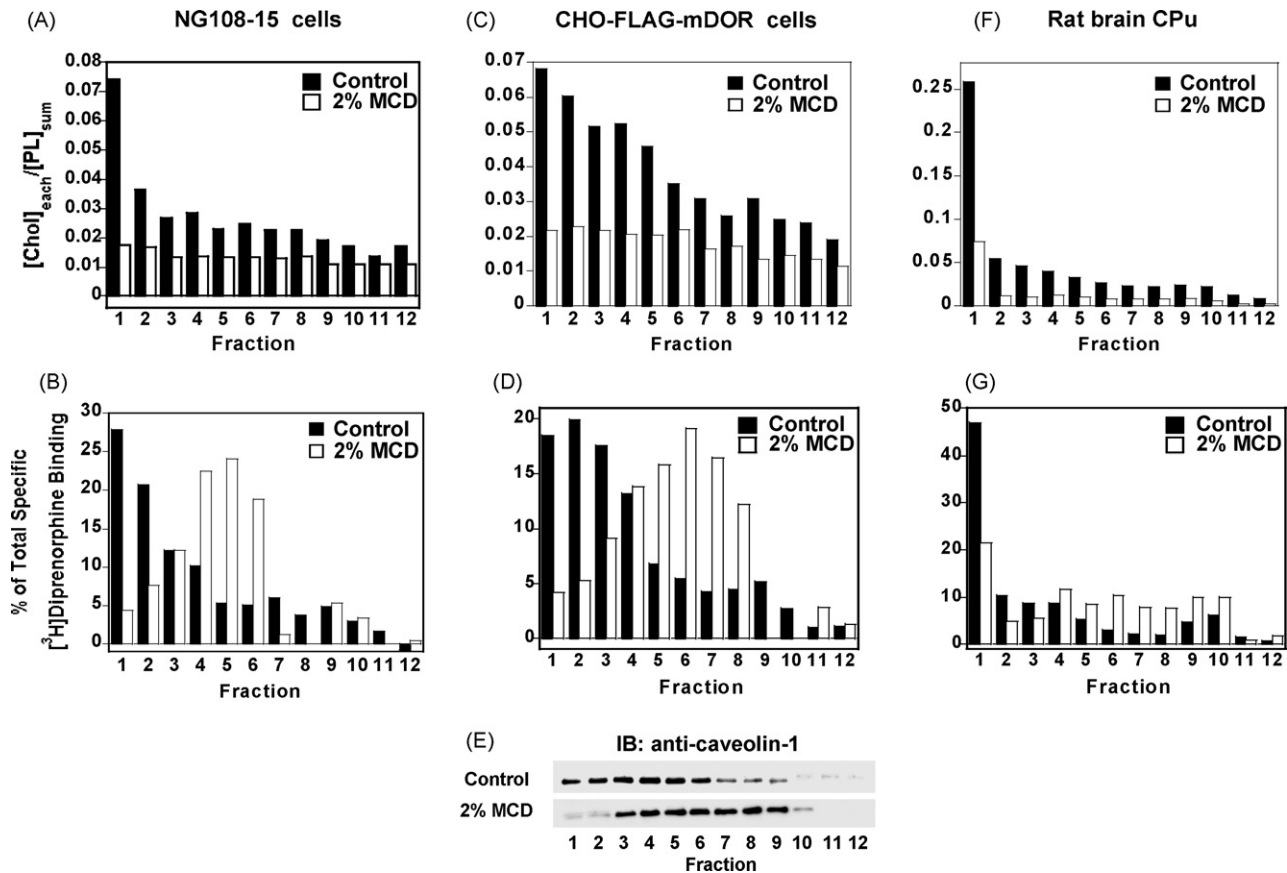
Fig. 6 – Effects of MCD treatment on cholesterol, DOR and caveolin-1 distribution in NG108-15 cells (A and B), CHO-FLAG-mDOR cells (C–E) and rat brain CPu membranes (F) (G). Tissues were treated with 2% MCD for 1 h at 37 °C as described in Section 2, then collected and subjected to lipid rafts preparation through continuous sucrose gradients. Twelve 1-ml fractions were collected and for each fraction (A, C and F) cholesterol contents were determined with data expressed as the ratios of [cholesterol in each fraction]/[total phospholipids]). (B, D and G) [^{3}H]diprenorphine-specific binding experiment was performed to detect DOR and data were expressed as % of total specific [^{3}H]diprenorphine binding. (E) Caveolin-1 immunoblotting with an anti-caveolin-1 monoclonal antibody. Each figure represents one of the two experiments performed with similar results.

value of DPDPE (>5-fold) and the K_d value of [^{3}H]diprenorphine binding (>2-fold) for the DOR. In CHO-FLAG-mDOR cells the treatment only slightly decreased the B_{max} value of [^{3}H]diprenorphine binding, whereas it decreased the B_{max} value in NG108-15 cells profoundly.

3.8. Effects of MCD treatment on DOR-mediated G protein activation

Activation of DOR enhances [^{35}S]GTPγS binding to pertussis toxin-sensitive G proteins in cell membranes [38], which has

Table 1 – Effects of MCD pre-treatment on K_d and B_{max} values of [^{3}H]diprenorphine binding and K_i values of DPDPE binding to DOR in membranes of CHO-FLAG-mDOR cells and NG108-15 cells

Cells	Ligands	Affinities and B_{max}	Control	MCD-treated
CHO	[^{3}H]dip	K_d (nM)	0.23 ± 0.01	0.49 ± 0.03[#]
		B_{max} (fmol/mg mem protein)	5844 ± 169	5159 ± 248[^]
	DPDPE	K_i (nM)	9.60 ± 0.76	55.8 ± 6.3[#]
NG108-15	[^{3}H]dip	K_d (nM)	0.25 ± 0.05	0.66 ± 0.11[*]
		B_{max} (fmol/mg mem protein)	571 ± 34	252 ± 30[#]
	DPDPE	K_i (nM)	22.4 ± 3.4	195 ± 60[*]

Cells were treated with vehicle or 2% MCD, cell membranes were prepared, saturation binding of [^{3}H]diprenorphine to cell membranes was performed and K_d and B_{max} values were calculated as described in Section 2. Competition inhibition by DPDPE of [^{3}H]diprenorphine binding was conducted and its K_i value was determined. Each value represents mean ± S.E.M. of three experiments performed in duplicate. [#]$P < 0.001$, [*]$P < 0.01$, [^]$P < 0.05$, by Student's two-tailed t tests, compared with each control.
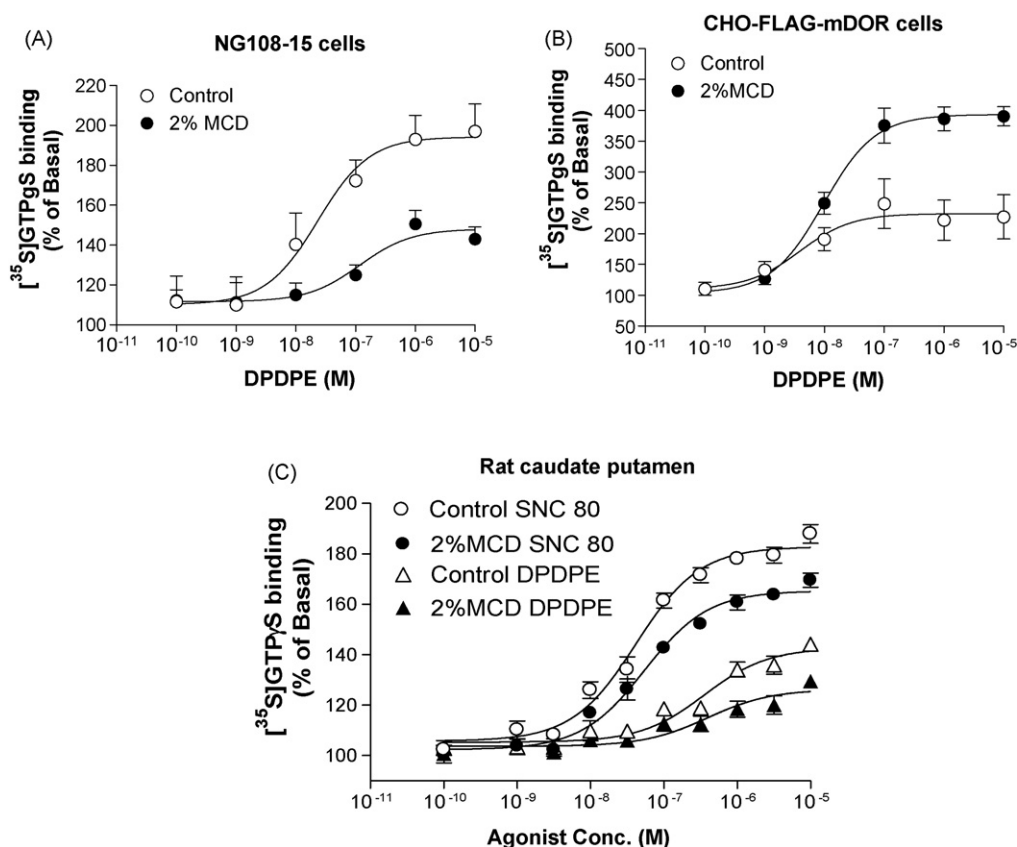
Fig. 7 – MCD pre-treatment has different effects on agonist-induced [^{35}S]GTPγS binding to membranes of (A) NG108-15 cells, (B) CHO-FLAG-mDOR cells and (C) rat brain CPu. Cells or rat CPu membranes were incubated with vehicle or 2% MCD, membranes were prepared and [^{35}S]GTPγS binding experiments were performed as described in Section 2. Data are shown as mean ± S.E.M. of three to five experiments performed in duplicate and summarized in Table 2.

been used as a functional measure for G protein activation. In NG108-15 cells, MCD treatment greatly reduced the E_{max} value of DPDPE and increased its EC_{50} value (Fig. 7A and Table 2). In rat CPu membranes, MCD treatment attenuated the E_{max} values of both DPDPE and SNC80, but did not change the EC_{50} values significantly (Fig. 7C and Table 2). In contrast, in CHO-FLAG-mDOR cells, MCD treatment greatly enhanced the E_{max} value of DPDPE without affecting its EC_{50} value

significantly (Fig. 7B and Table 2). The EC_{50} values of DPDPE for DORs in the three tissues are different: CPu ≫ NG108-15 ≫ CHO. Our results are consistent with the findings of Szekeres and Traynor for NG108-15 cells [38] and those of Unterwald and Cuntapay [39] and Sim et al. [40] for CPu membranes. The discrepancies may be due to different levels of receptors [41] and G proteins and their stoichiometry in different tissues.

Table 2 – Effects of MCD pre-treatment on EC_{50} and E_{max} values of delta agonists in stimulating [^{35}S]GTPγS binding to membranes of CHO-FLAG-mDOR cells, NG108-15 cells and rat CPu

	Control		2% MCD-treated	
	EC_{50} (nM)	E_{max} (% of basal)	EC_{50} (nM)	E_{max} (% of basal)
CHO-FLAG-mDOR cells				
DPDPE	3.9 ± 3.1	232 ± 15.5	9.6 ± 3.0	393 ± 10.2[#]
NG108-15 cells				
DPDPE	23 ± 2.0	194 ± 8.5	167 ± 2.6[#]	148 ± 5.5[*]
Rat caudate putamen				
SNC 80	39 ± 5.7	183 ± 2.3	54 ± 7.6	165 ± 2.2[*]
DPDPE	364 ± 100	144 ± 2.8	271 ± 77	128 ± 4.7[^]

Cells were incubated with vehicle or 2% MCD, membranes were prepared and [^{35}S]GTPγS binding experiments were performed as described in Section 2. Data are shown as mean ± S.E.M. of three to five experiments performed in duplicate. [#]$P < 0.001$, [*]$P < 0.01$, [^]$P < 0.05$, by Student's two-tailed t tests, compared with each control.
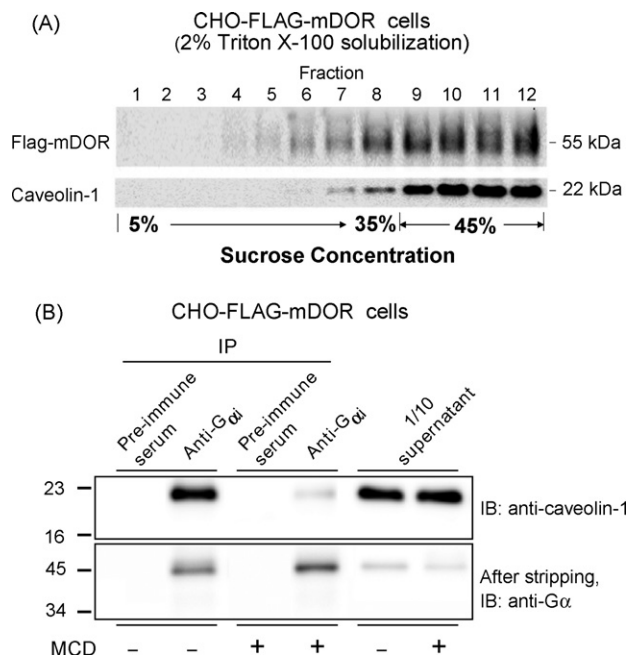
Fig. 8 – (A) Solubilization of CHO-FLAG-mDOR cells by 2% Trition X-100. Cells were solubilized at 4 °C for 1 h in buffer A containing 2% Triton X-100, 50 mM Tris–HCl (pH 7.4) and 1 μM PMSF, and then centrifuged at 100,000 × g for 1 h. The 2-ml supernatant was mixed with 2 ml of 90% sucrose prepared in buffer A, yielding 45% sucrose in a total volume of 4 ml. An 8-ml continuous gradient of 5–35% sucrose prepared in buffer A was layered on the top of the 45% fraction. Isopycnic ultracentrifugation were then carried out at 39,000 rpm (~190,000 × g) using a Beckman ultracentrifuge and a SW 41 rotor for 16–20 h at 4 °C. Following ultracentrifugation, twelve 1-ml fractions were collected from the bottom of the gradient tube using a peristaltic pump (RAININ). FLAG-mDOR and caveolin-1 in each fraction were examined by Western blot as mentioned in Section 2. (B) Co-immunoprecipitation of $G_{\alpha i}$ proteins and caveiolin-1 in CHO-FLAG-mDOR cells was reduced by MCD treatment. Cells were treated with vehicle or 2% MCD and harvested as described under Section 2. Cells were solubilized with 2% Triton X-100 and then centrifuged at 100,000 × g. The supernatant was incubated with rabbit anti-$G_{\alpha i\text{-}3}$ antibody, which recognizes all $G_{\alpha i}$ proteins, or normal rabbit serum and then with Protein A/G PLUS-Agarose. Immunoprecipitated materials were dissolved in 2× Laemmli loading buffer, resolved in 10% SDS-PAGE and transferred to Immobilon-P PVDF membranes. Immunoblotting was performed with a monoclonal antibody against caveolin-1 (top panel). One-tenth of the supernatant was resolved and blotted as well. The membranes were then stripped and blotted again with the rabbit anti-$G_{\alpha i\text{-}3}$ antibody (bottom panel). The figures represent one of the three experiments performed with similar results.

3.9. Co-immunoprecipitation of caveolin-1 with $G_{\alpha i}$ proteins in CHO cells was attenuated by MCD treatment

The differences in the MCD effects on DOR signaling in neuronal and non-neuronal cells may be attributed, at least in part, to the differential expression of caveolin-1 and its associated effects on activities of G proteins. We thus tested the hypothesis that caveolin-1 interacts with $G_{\alpha i}$ proteins and MCD affects the interaction. CHO-FLAG-mDOR cells were solubilized with 2% Triton X-100 and centrifuged at 100,000 × g for 1 h. In the literature, Trition X-100 concentration used to solubilize non-rafts membranes and, thus, define lipid rafts, ranged from 0.1% to 1%. To assess the completeness of 2% Triton X-100 solubilization used for immunoprecipitation, we fractionated the 100,000 × g supernatant in the 5–35% continuous sucrose gradient. The vast majority of FLAG-mDOR and caveolin-1 immunoreactivities were detected in the fractions 8–12 (Fig. 8A). These results indicate that the solubilization is successful and demonstrate that buoyancy of rafts DOR is not an inherent property of the protein, rather, a reflection of its membrane environment. $G_{\alpha i}$ proteins were immunoprecipitated from the supernatant with anti-$G_{\alpha i}$ antibodies, but not with pre-immune serum (Fig. 8B, lower panel). Caveolin-1 co-immunoprecipitated with $G_{\alpha i}$ proteins and 2% MCD-pre-treatment reduced the amount of caveolin-1 co-immunoprecipitated with $G_{\alpha i}$ proteins (Fig. 8B, upper panel).

4. Discussion

To the best of our knowledge, the findings that opioid receptors in rat brain CPu membranes and the DOR in NG108-15 cells are mainly present in lipid rafts and full agonists move some of the receptors out of lipid rafts represent the first report to study the relationship between a GPCR and non-caveolae rafts in neuronal cells. The present study reveals that localization of a GPCR in lipid rafts or agonist-promoted shift of the GPCR out of lipid rafts is independent of caveolin-1. In addition, this is also the first demonstration that cholesterol depletion has opposite effects on signaling of the same GPCR in brain membranes and a neuron-like cell line vs. a non-neuronal cell line. These findings suggest that cholesterol-dependent association of caveolin-1 with $G_{\alpha i}$ might play an important role in inhibiting Gi/o-coupled GPCRs-mediated G protein activation in caveolin-1-enriched cells.

4.1. Physiological and pharmacological relevance of lipid rafts

Lipid rafts appear to serve as a platform to organize signaling molecules, at least the δ receptor and G proteins. In neuronal cells, such an organization facilitates signaling, whereas in non-neuronal cells it appears to constrain signaling, perhaps due to the presence of caveolins. Although the majority of the δ opioid receptor is localized in lipid rafts, some are not. Since cholesterol contents in membranes influence receptor properties as observed in this study, it is possible that the receptors in lipid rafts may have different functional properties from those outside of lipid rafts.

4.2. Lipid rafts as low-density membrane domains: what is the density limit?

Brown and Rose [10] first reported that most of the GPI-anchored human placental alkaline phosphatase were found in membranes at a density of 1.081 g/cc or lower, which were located in middle fractions in a linear 5–30% sucrose density gradient and corresponded to up to ∼20% sucrose. Macdonald and Pike [35] defined that raft fractions as those with a concentration range of 0–5% Optiprep plus ∼9% sucrose, which had a similar density limit as what Brown and Rose described. Thus, in this study, rafts fractions are referred to those fractions with densities equal to or lower than 20% sucrose, i.e. fractions 1–4 of the 5–35% continuous sucrose gradient. It is noteworthy that, based on this definition, some caveolin-1 proteins are located out of lipid rafts in CHO cells (Figs. 5C or 6E, control). Similarly, Pike and colleagues reported that caveolin was recovered in fractions of a significantly higher density than other raft marker proteins and cholesterol [35]. It was suggested that incomplete disruption of caveolae/actin association might result in the generation of relatively heavy caveolae membranes [35]. The subtle density differences among such heterogeneous rafts populations were obscured when the commonly used 5%/35%/45% discontinuous sucrose gradient was employed to prepare lipid rafts (e.g., Fig. 3B, middle and lower panels).

4.3. Agonist-induced shift of DOR

That DOR expressed in CHO cells was predominantly localized in lipid rafts is similar to the findings that the majority of μ [22] and κ [21] opioid receptors were distributed in lipid rafts in heterologous expression systems enriched in caveolin-1. In addition, the μ and δ opioid receptors are localized in caveolae in cardiac myocytes, which are enriched in caveolin-3 [23,24].

[3H]diprenorphine binding was largely unaffected during the rafts preparation procedure, allowing determination of the distribution of opioid receptors quantitatively. In CHO cells, the distribution profile of FLAG-DOR protein immunoreactivity in fractions was similar to that of [3H]diprenorphine binding, indicating that the lack of binding in higher sucrose density fractions following detergent-free preparation procedure is due to the absence of receptor, but not loss of binding activity in these fractions. To the best of our knowledge, there are no good antibodies for immunoblotting of endogenous DOR.

Treatment of cells with full agonists moved some DOR out of lipid rafts into higher density fractions. These fractions may represent non-rafts plasma membranes and/or endosomal membranes.

The DOR is similar to some GPCRs, for example β2-adrenergic receptors, that are constitutively localized in lipid rafts and, upon agonist binding, some moved out of rafts [42]. In contrast, some GPCRs completely or partially reside outside of lipid rafts, and are moved into the lipid rafts by, such as bradykinin B2 receptor [43]. In addition, the lipid rafts partitioning of some other GPCRs is not affected by agonist stimulation, for example, endothelin ETA receptor [44]. The mechanisms for the different behaviors of GPCRs are not clear.

Using plasmon-waveguide resonance spectroscopy, Alves et al. reported that in a model membrane system, the DOR was largely incorporated into palmitoyloleoyl phosphatidylcholine-rich membrane domain, whereas in the presence of a ligand, the receptor was preferentially incorporated into sphingomyelin-rich domain [45]. An agonist has a two-fold greater propensity than an antagonist in inducing the shift [45]. These studies indicate that partitioning of DOR into different lipid micro-environments does occur and such differential localization depends on ligand-induced states of the receptor.

4.4. Does DOR need to shift out of lipid rafts to be internalized?

Internalization of the DOR has been observed to require receptor activation and involve clathrin-coated pits in mammalian cells [46], which reaches a plateau in 30 min [47] and is unaffected by PTX treatment [48]. The full agonist-induced DOR shift out of lipid rafts at 30 min depends on receptor activation, but not $G_{i/o}$ protein activation. In addition, DOR has been shown not to be internalized by levorphanol [49] and morphine [50]. There was no shift observed when NG108-15 cells were treated with levorphanol and morphine at 10 μM. All agonist concentrations used are saturating concentrations for the DOR. Thus, there is an interesting parallel between agonist-induced internalization and shift out of lipid rafts. Both membrane-impermeable peptide agonists (DPDPE and deltorphin II) and the membrane-permeable non-peptide agonist (etorphine) shifted some DOR out of rafts, indicating that the shifted portion of DOR is originally located in plasma membranes rather than intracellular compartments. Thus, it is plausible that getting out of lipid rafts is an initial step for DOR internalization. Alternatively, DOR may be internalized first and then translocated to a non-raft subcellular compartment. Detailed mechanisms are under investigation. The β2-adrenergic receptor has been proposed to leave lipid rafts to be internalized via clathrin-coated pits following agonist treatment [42,51]. In contrast, agonist-promoted movements of μ opioid receptors out of lipid rafts appear to be unrelated to internalization, since morphine and etorphine cause similar extents of shift out of lipid rafts, although etorphine, but not morphine, promotes internalization of the μ receptor [22].

4.5. Cholesterol is an important factor for localization of DOR in lipid rafts and for maintaining ligand binding affinities to DOR

Lawrence et al. showed by atomic force microscopy that lipid rafts in model lipid bilayers were patch-like and MCD treatment diminished and eventually disrupted lipid rafts in a time-dependent manner [52]. It is conceivable that similar processes occur in cell membranes upon cholesterol reduction. In both NG108-15 cells and CHO-FLAG-mDOR cells, DOR was shifted out of lipid rafts fractions into higher density fractions upon 2%MCD treatment, which reduced cholesterol by ∼50%. Caveolin-1 showed a similar shift. Furthermore, the same MCD treatment significantly decreased the binding affinities of both the full agonist DPDPE and the antagonist diprenorphine, suggesting that the cholesterol-rich membrane micro-environments in lipid rafts are required to maintain proper conformations of the DOR in both cell lines.

Interestingly, the same MCD treatment did not affect the rafts distribution of flotillin-1 in some cells [21,53]. Moreover, depletion of sphingolipids did not change the localization of rafts-associated DOR in NG108-15 cells (our unpublished observation). Thus, although we have not shown directly that cholesterol and DOR are associated in cells prior to lysis, our observations regarding DOR-rafts relationships would be expected to implicate a cholesterol–DOR complex.

It is noteworthy that although the human κ opioid receptor expressed in CHO cells was shifted out of low-density fractions in a similar manner as DOR following ∼50% cholesterol reduction, MCD did not change the affinity of diprenorphine, and even significantly increased the affinity of the full agonist U50,488H to the κ receptor [21], suggesting that localization in lipid rafts has different impacts on the functional properties of the κ and δ opioid receptors.

Changes in cholesterol contents of brain membranes have been shown in animals under certain physiological or pathological conditions. For example, cholesterol delivery from astrocytes to neurons is required for synapse formation, and membrane cholesterol contents increased sharply at the time of delivery [54]. In addition, cholesterol-to-phospholipid ratio of brain synaptic plasma membranes was significantly lower in LDL receptor-deficient mice [55]. Thus, varying cholesterol contents in cell membranes may affect opioid receptor functional properties in brain.

4.6. Possible mechanisms underlying the difference in MCD treatment-induced changes in DOR signaling between CHO-FLAG-mDOR cells vs. NG108-15 cells and rat brains: the role of caveolin-1

Since the agonist affinities to DOR were decreased by cholesterol reduction in both cells lines, it was expected that DPDPE-induced G protein activation was attenuated by MCD treatment, which was the case in NG108-15 cells and rat CPu membranes. However, in CHO-FLAG-mDOR cells the efficacy of DPDPE-induced G protein activation was profoundly increased and the potency was unchanged by MCD treatment.

A membrane rafts-related difference among the two cell lines and rat CPu membranes is the level of caveolin-1, which was abundant in CHO cells, but undetectable in NG108-cells and very low in rat brain. That the rat brain had a very low level of caveolin-1 is consistent with the findings of Cameron et al. [26] and Wu et al. [56]. However, the possibility cannot be ruled out that subpopulations of neurons may express significant levels of caveolin-1 at different developmental stage. In addition, the finding of Lang et al. [57] and our unpublished observation showed that there were no caveolin-1 immuno-staining in dorsal root ganglia neurons, which express high levels of opioid receptors.

In vitro, recombinant caveolin-1 interacts with α subunits of G_s, G_o or G_i proteins directly, and potently inhibited activities of G_α proteins [58]. In addition, incorporation of recombinant caveolin-1 into phosphatidylcholine-based membranes was greatly increased by cholesterol, and the reconstituted caveolin-1-containing membranes were capable of recruiting a soluble recombinant form of $G_{\alpha i2}$ [59]. Furthermore, stable transfection of caveolin-1 or -3 into NG108-15 cells attenuated

inhibition of N-type voltage-gated Ca^{2+} channels mediated by DOR or by direct stimulation of G proteins [60].

Here we have demonstrated that, in CHO-FLAG-mDOR cells, caveolin-1 co-immunoprecipitates with $G_{\alpha i}$ proteins, similar to the results in several studies (for example, [43,61]). MCD pre-treatment substantially decreased the amount of caveolin-1 co-immunoprecipitated with $G_{\alpha i}$ proteins, which presumably releases some inhibitory effect of caveolin-1 on the activities of $G_{\alpha i}$ proteins. This disinhibition apparently overcomes the loss of agonist affinity induced by MCD treatment, resulting in the higher degree of DOR-mediated $G_{\alpha i/o}$ protein activation. Similar to our finding, cholesterol reduction resulted in enhancement of agonist-stimulated [^{35}S]GTPγ binding mediated by the κ opioid receptors in CHO cells [21] and the CB1 cannabinoid receptor in rat C6 glioma cells [62]. Both cell lines express high levels of caveolin-1. Therefore, cholesterol-dependent association of caveolin-1 with $G_{\alpha i}$ may be important in regulating $G_{i/o}$-coupled GPCRs-mediated G protein activation. This hypothesis is supported by the finding that the association of caveolin-1 with the transducin α subunit in bovine photoreceptor rod outer segments was disrupted by cyclodextrin treatment or being exposed to light in the presence of GTPγS [63].

However, such a scenario is not likely to occur in neurons, such as NG108-15 cells, due to the absence or low level of caveolin-1. Thus, since DOR is mainly distributed in neurons in brain, cholesterol depletion reduced DOR-induced G protein activation in rat CPu membranes.

The possibility that the difference may be due to over-expressed δ receptor in CHO cells vs. endogenous δ receptor cannot be excluded. We performed [^{3}H]diprenorphine binding on membrane preparations of the rat heart, which has high levels of caveolins. Unfortunately, [^{3}H]diprenorphine-specific binding was barely above the background. Based on our experiences, it was not possible to obtain [^{35}S]GTPγS binding signal when receptor binding was so low. We know of no other system that we can use for this purpose.

4.7. MCD effects

The direct effect of MCD on cells is extraction of cholesterol in the outer layer of plasma membranes. Cholesterol reduction by MCD indirectly may alter cell structure and membrane properties in several ways, including disrupting lipid rafts, altering plasma membrane lipid asymmetry, modifying cytoskeletal structure and changing membrane fluidity. In our previous study, we found 2% MCD did not affect cell viability [21]. Pre-treatment with 2% MCD followed by MCD-conjugated cholesterol restored cell cholesterol contents and reversed all the MCD effects, including localization of the κ receptor in lipid rafts and returning the receptor-mediated G protein activation to control level, indicating that MCD effects are due to reduction in cholesterol [21]. The focus of our present study is to examine how MCD-induced cholesterol changes in lipid rafts are correlated with the changes in the location and function of delta opioid receptors, which is an important step toward a better understanding of opioid receptor–membrane interactions in both neuronal and non-neuronal cells.

However, we do not exclude the possibility that the observed changes in opioid receptors are related to other

MCD-induced changes in cell structure or membrane properties. Cholesterol extraction leads to decreases in the lateral diffusion coefficients of proteins and lipids within plasma membranes [64,65], which have been attributed to membrane lateral reorganization (e.g., presence of solid-like lipid regions [65]) and reorganization of actin [64].

4.8. Conclusion

DOR primarily partitions into lipid rafts in brain membranes, NG108-15 cells and CHO cells, independent of the level of caveolin-1. Treatment with full agonists shifts a portion of DOR out of lipid rafts, which may undergo internalization. Reduction of cholesterol level significantly attenuated DOR-mediated G protein activation in rat brain and NG108-15 cells, but enhanced it in CHO cells in spite of the similar decrease in the agonist affinity by the treatment in both cell lines. The differences might be due to the presence of high level of caveolin-1, which inhibits G proteins, in CHO cells, but not in rat brain and NG108-15 cells. Cholesterol reduction decreased the association between caveolin-1 and $G_{\alpha i}$ proteins, which may lead to disinhibition of $G_{\alpha i}$ and the observed enhancement in signaling in CHO cells.

Acknowledgments

Appendix A. Supplementary data

Supplementary data associated with this article can be found, in the online version, at doi:10.1016/j.bcp.2006.10.032.

REFERENCES

[1] Zhu Y, King MA, Schuller AG, Nitsche JF, Reidl M, Elde RP, et al. Retention of supraspinal delta-like analgesia and loss of morphine tolerance in delta opioid receptor knockout mice. Neuron 1999;24:243–52.

[2] Filliol D, Ghozland S, Chluba J, Martin M, Matthes HW, Simonin F, et al. Mice deficient for delta- and mu-opioid receptors exhibit opposing alterations of emotional responses. Nat Genet 2000;25:195–200.

[3] Rapaka RS, Porreca F. Development of delta opioid peptides as nonaddicting analgesics. Pharm Res 1991;8:1–8.

[4] Schultz JJ, Hsu AK, Gross GJ. Ischemic preconditioning and morphine-induced cardioprotection involve the delta (delta)-opioid receptor in the intact rat heart. J Mol Cell Cardiol 1997;29:2187–95.

[5] Bell SP, Sack MN, Patel A, Opie LH, Yellon DM. Delta opioid receptor stimulation mimics ischemic preconditioning in human heart muscle. J Am Coll Cardiol 2000;36:2296–302.

[6] Gross GJ. Role of opioids in acute and delayed preconditioning. J Mol Cell Cardiol 2003;35:709–18.

[7] Peart JN, Gross ER, Gross GJ. Opioid-induced preconditioning: recent advances and future perspectives. Vascul Pharmacol 2005;42:211–8.

[8] Law P-Y, Wong YH, Loh HH. Molecular mechanisms and regulation of opioid receptor signaling. Ann Rev Pharmacol Toxicol 2000;40:389–430.

[9] Pike LJ. Rafts defined: a report on the Keystone Symposium on Lipid Rafts and Cell Function. J Lipid Res 2006;47:1597–8.

[10] Brown DA, Rose JK. Sorting of GPI-anchored proteins to glycolipid-enriched membrane subdomains during transport to the apical cell surface. Cell 1992;68:533–44.

[11] Shaw AS. Lipid rafts: now you see them, now you don't. Nat Immunol 2006;7:1139–42.

[12] Cohen AW, Hnasko R, Schubert W, Lisanti MP. Role of caveolae and caveolins in health and disease. Physiol Rev 2004;84:1341–79.

[13] Razani B, Woodman SE, Lisanti MP. Caveolae: from cell biology to animal physiology. Pharmacol Rev 2002;54:431–67.

[14] Pike LJ. Lipid rafts: bringing order to chaos. J Lipid Res 2003;44:655–67.

[15] Chini B, Parenti M. G-protein coupled receptors in lipid rafts and caveolae: how, when and why do they go there? J Mol Endocrinol 2004;32:325–38.

[16] Okamoto T, Schlegel A, Scherer PE, Lisanti MP. Caveolins, a family of scaffolding proteins for organizing "preassembled signaling complexes" at the plasma membrane. J Biol Chem 1998;273:5419–22.

[17] Ostrom RS, Insel PA. The evolving role of lipid rafts and caveolae in G protein-coupled receptor signaling: implications for molecular pharmacology. Br J Pharmacol 2004;143:235–45.

[18] Law PY, Nicksic TD, O'Rourke MA, Koehler JE, Herz A, Loh HH. Potentiation of opiate action in neuroblastoma N18TG2 cells by lipid incorporation. Mol Pharmacol 1982;21:492–502.

[19] Rao BG, Murphy MG. Opiate peptide receptors on intact NIE-115 neuroblastoma: radioligand binding properties, intracellular response, and effects of increasing membrane cholesterol. Prog Neuropsychopharmacol Biol Psychiatry 1984;8:719–23.

[20] Hasegawa J, Loh HH, Lee NM. Lipid requirement for mu opioid receptor binding. J Neurochem 1987;49:1007–12.

[21] Xu W, Yoon SI, Huang P, Wang Y, Chen C, Chong PL, et al. Localization of the kappa opioid receptor in lipid rafts. J Pharmacol Exp Ther 2006; 317:1295–306.

[22] Zhao H, Loh HH, Law PY. Adenylyl cyclase superactivation induced by long-term treatment with opioid agonist is dependent on receptor localized within lipid rafts and is independent of receptor internalization. Mol Pharmacol 2006;69:1421–32.

[23] Head BP, Patel HH, Roth DM, Lai NC, Niesman IR, Farquhar MG, et al. G-protein-coupled receptor signaling components localize in both sarcolemmal and intracellular caveolin-3-associated microdomains in adult cardiac myocytes. J Biol Chem 2005;280:31036–44.

[24] Patel HH, Head BP, Petersen HN, Niesman IR, Huang D, Gross GJ, et al. Protection of adult rat cardiac myocytes from ischemic cell death: role of caveolar microdomains and delta opioid receptors. Am J Physiol Heart Circ Physiol 2006;291:H344–50.

[25] Couet J, Li S, Okamoto T, Ikezu T, Lisanti MP. Identification of peptide and protein ligands for the caveolin-scaffolding domain. Implications for the interaction of caveolin with caveolae-associated proteins. J Biol Chem 1997;272:6525–33.

[26] Cameron PL, Ruffin JW, Bollag R, Rasmussen H, Cameron RS. Identification of caveolin and caveolin-related proteins in the brain. J Neurosci 1997;17:9520–35.

[27] Chen C, Xue JC, Zhu J, Chen YW, Kunapuli S, de Riel JK, et al. Characterization of irreversible binding of beta-funaltrexamine to the cloned rat mu opioid receptor. J Biol Chem 1995;270:17866–70.

[28] Song KS, Li S, Okamoto T, Quilliam LA, Sargiacomo M, Lisanti MP. Co-purification and direct interaction of Ras with caveolin, an integral membrane protein of caveolae microdomains. Detergent-free purification of caveolae microdomains. J Biol Chem 1996;271:9690–7.

[29] Bartlett GR. Phosphorus assay in column chromatography. J Biol Chem 1959;234:466–8.

[30] Li J, Chen C, Huang P, Liu-Chen L-Y. Inverse agonist up-regulates the constitutively active D3.49(164)Q mutant of the rat (opioid receptor by stabilizing the structure and blocking constitutive internalization and down-regulation. Mol Pharmacol 2001;60:1064–75.

[31] Zhu J, Luo L-Y, Chen C, Liu-Chen L-Y. Activation of the cloned human κ opioid receptor by agonists enhances [^{35}S]GTPγS binding to membranes: Determination of potencies and efficacies of ligands. J Pharmacol Exp Ther 1997;282:676–84.

[32] Zhu J, Luo LY, Mao GF, Ashby B, Liu-Chen L-Y. Agonist-induced desensitization and down-regulation of the human kappa opioid receptor expressed in CHO cells. J Pharmacol Exp Ther 1998;285:28–36.

[33] Huang P, Kehner GB, Cowan A, Liu-Chen L-Y. Comparison of pharmacological activities of buprenorphine and norbuprenorphine: norbuprenorphine is a potent opioid agonist. J Pharmacol Exp Ther 2001;297:688–95.

[34] Mansour A, Khachaturian H, Lewis ME, Akil H, Watson SJ. Anatomy of CNS opioid receptors. Trends Neurosci 1988;11:308–14.

[35] Macdonald JL, Pike LJ. A simplified method for the preparation of detergent-free lipid rafts. J Lipid Res 2005;46:1061–7.

[36] Kilsdonk EP, Yancey PG, Stoudt GW, Bangerter FW, Johnson WJ, Phillips MC, et al. Cellular cholesterol efflux mediated by cyclodextrins. J Biol Chem 1995;270:17250–6.

[37] Rothberg KG, Heuser JE, Donzell WC, Ying YS, Glenney JR, Anderson RG. Caveolin, a protein component of caveolae membrane coats. Cell 1992;68:673–82.

[38] Szekeres PG, Traynor JR. Delta opioid modulation of the binding of guanosine-5′-O-(3-[35S]thio)triphosphate to NG108-15 cell membranes: characterization of agonist and inverse agonist effects. J Pharmacol Exp Ther 1997;283:1276–84.

[39] Unterwald EM, Cuntapay M. Dopamine-opioid interactions in the rat striatum: a modulatory role for dopamine D1 receptors in delta opioid receptor-mediated signal transduction. Neuropharmacol 2000;39:372–81.

[40] Sim LJ, Selley DE, Xiao R, Childers SR. Differences in G-protein activation by mu- and delta-opioid, and cannabinoid, receptors in rat striatum. Eur J Pharmacol 1996;307:97–105.

[41] Whaley BS, Yuan N, Birnbaumer L, Clark RB, Barber R. Differential expression of the beta-adrenergic receptor modifies agonist stimulation of adenylyl cyclase: a quantitative evaluation. Mol Pharmacol 1994;45:481–9.

[42] Rybin VO, Xu X, Lisanti MP, Steinberg SF. Differential targeting of beta-adrenergic receptor subtypes and adenylyl cyclase to cardiomyocyte caveolae. A mechanism to functionally regulate the cAMP signaling pathway. J Biol Chem 2000;275:41447–5.

[43] De Weerd WF, Leeb-Lundberg LM. Bradykinin sequesters B2 bradykinin receptors and the receptor-coupled Galpha subunits Galphaq and Galphai in caveolae in DDT1 MF-2 smooth muscle cells. J Biol Chem 1997;272:17858–66.

[44] Chun M, Liyanage UK, Lisanti MP, Lodish HF. Signal transduction of a G protein-coupled receptor in caveolae: colocalization of endothelin and its receptor with caveolin. Proc Natl Acad Sci USA 1994;91:11728–32.

[45] Alves ID, Salamon Z, Hruby VJ, Tollin G. Ligand modulation of lateral segregation of a G-protein-coupled receptor into lipid microdomains in sphingomyelin/phosphatidylcholine solid-supported bilayers. Biochemistry 2005;44:9168–78.

[46] Varga EV, Navratilova E, Stropova D, Jambrosic J, Roeske WR, Yamamura HI. Agonist-specific regulation of the delta-opioid receptor. Life Sci 2004;76:599–612.

[47] Chu P, Murray S, Lissin D, von Zastrow M. Delta and kappa opioid receptors are differentially regulated by dynamin-dependent endocytosis when activated by the same alkaloid agonist. J Biol Chem 1997;272:27124–30.

[48] Eisinger DA, Ammer H, Schulz R. Chronic morphine treatment inhibits opioid receptor desensitization and internalization. J Neurosci 2002;22:10192–200.

[49] Bot G, Blake AD, Li S, Reisine T. Opioid regulation of the mouse delta-opioid receptor expressed in human embryonic kidney 293 cells. Mol Pharmacol 1997;52:272–81.

[50] Zhang J, Ferguson SS, Law P-Y, Barak LS, Caron MG. Agonist-specific regulation of delta-opioid receptor trafficking by G protein-coupled receptor kinase and beta-arrestin. J Receptor Signal Trans Res 1999;19:301–13.

[51] Schwencke C, Okumura S, Yamamoto M, Geng YJ, Ishikawa Y. Colocalization of beta-adrenergic receptors and caveolin within the plasma membrane. J Cell Biochem 1999;75:64–72.

[52] Lawrence JC, Saslowsky DE, Edwardson JM, Henderson RM. Real-time analysis of the effects of cholesterol on lipid raft behavior using atomic force microscopy. Biophys J 2003;84:1827–32.

[53] Rajendran L, Masilamani M, Solomon S, Tikkanen R, Stuermer CA, Plattner H, et al. Asymmetric localization of flotillins/reggies in preassembled platforms confers inherent polarity to hematopoietic cells. Proc Natl Acad Sci USA 2003;100:8241–6.

[54] Mauch DH, Nagler K, Schumacher S, Goritz C, Muller EC, Otto A, et al. CNS synaptogenesis promoted by glia-derived cholesterol. Science 2001;294:1354–7.

[55] Igbavboa U, Avdulov NA, Chochina SV, Wood WG. Transbilayer distribution of cholesterol is modified in brain synaptic plasma membranes of knockout mice deficient in the low-density lipoprotein receptor, apolipoprotein E, or both proteins. J Neurochem 1997;69:1661–7.

[56] Wu C, Butz S, Ying Y, Anderson RG. Tyrosine kinase receptors concentrated in caveolae-like domains from neuronal plasma membrane. J Biol Chem 1997;272:3554–9.

[57] Lang DM, Lommel S, Jung M, Ankerhold R, Petrausch B, Laessing U, et al. Identification of reggie-1 and reggie-2 as plasmamembrane-associated proteins which cocluster with activated GPI-anchored cell adhesion molecules in non-caveolar micropatches in neurons. J Neurobiol 1998;37:502–23.

[58] Li S, Okamoto T, Chun M, Sargiacomo M, Casanova JE, Hansen SH, et al. Evidence for a regulated interaction between heterotrimeric G proteins and caveolin. J Biol Chem 1995;270:15693–701.

[59] Li S, Song KS, Lisanti MP. Expression and characterization of recombinant caveolin. Purification by polyhistidine tagging and cholesterol-dependent incorporation into defined lipid membranes. J Biol Chem 1996;271:568–73.

[60] Toselli M, Taglietti V, Parente V, Flati S, Pavan A, Guzzi F, et al. Attenuation of G protein-mediated inhibition of N-type calcium currents by expression of caveolins in mammalian NG108-15 cells. J Physiol 2001;536:361–73.

[61] Murthy KS, Makhlouf GM. Heterologous desensitization mediated by G protein-specific binding to caveolin. J Biol Chem 2000;275:30211–9.

[62] Bari M, Battista N, Fezza F, Finazzi-Agro A, Maccarrone M. Lipid rafts control signaling of type-1 cannabinoid receptors in neuronal cells. Implications for anandamide-induced apoptosis. J Biol Chem 2005;280:12212–20.

[63] Elliott MH, Fliesler SJ, Ghalayini AJ. Cholesterol-dependent association of caveolin-1 with the transducin alpha subunit in bovine photoreceptor rod outer segments: disruption by cyclodextrin and guanosine 5′-O-(3-thiotriphosphate). Biochemistry 2003;42:7892–903.

[64] Kwik J, Boyle S, Fooksman D, Margolis L, Sheetz MP, Edidin M. Membrane cholesterol, lateral mobility, and the phosphatidylinositol 4,5-bisphosphate-dependent organization of cell actin. Proc Natl Acad Sci USA 2003;100:13964–9.

[65] Nishimura SY, Vrljic M, Klein LO, McConnell HM, Moerner WE. Cholesterol depletion induces solid-like regions in the plasma membrane. Biophys J 2006;90:927–38.